

IJS-TP-98/01  
TECHNION-PH-98-01  
hep-ph/9801279

## Long distance contributions in $D \rightarrow V\gamma$ decays

S. Fajfer<sup>a</sup>, S. Prelovšek<sup>a</sup> and P. Singer<sup>b</sup>

*a) J. Stefan Institute, Jamova 39, P. O. Box 300, 1001 Ljubljana, Slovenia*

*b) Department of Physics, Technion - Israel Institute of Technology, Haifa  
32000, Israel*

### ABSTRACT

Using the factorization scheme for the nonleptonic  $D \rightarrow VV_0$  weak amplitudes, we classify all diagrams which arise in  $D \rightarrow V\gamma$  decays and calculate them with the help of the hybrid model which combines the heavy quark effective theory and the chiral Lagrangian approach. Thus we determine the long distance contribution to the amplitudes of Cabibbo allowed and Cabibbo suppressed  $D \rightarrow V\gamma$  decays. The calculation of the expected range of the branching ratios of nine different  $D \rightarrow V\gamma$  channels is compared with results of other approaches. The present work establishes an increase of the parity violating contribution in these decays in comparison with previous analyses.

## 1 Introduction

The study of nonleptonic decays of charm mesons has been a subject of high priority for more than two decades and has resulted in a wealth of experimental data, which continues to expand at a remarkable rate. This rich source of information plays a decisive role in the development of the theoretical treatment of these processes, which are governed by the interplay of the weak and strong interactions.

On the other hand, there is very little information available on the sector of flavour changing radiative decays of charm mesons, in which the electromagnetic interactions is also operative.

Only some preliminary upper limits, at the  $10^{-4}$  range, for branching ratios of Cabibbo forbidden decays of type  $D^0 \rightarrow V^0\gamma$  have been reported so far [1]. However, as a result of ongoing efforts [2] it is reasonable to expect that the experimental data on  $D \rightarrow V\gamma$  decays will be forthcoming during the next few years. The theoretical treatment of these decays must address firstly the question of the relative importance of short and long distance contributions. For the decays studied here, the short distance process of relevance, the  $c \rightarrow u\gamma$  transition which is driven by the magnetic penguin diagram, is exceedingly small being suppressed by GIM cancellation and small CKM matrix elements [3]. The inclusion of gluonic corrections [3, 4] increases the free quark  $c \rightarrow u\gamma$  amplitude by several orders of magnitude. However, even after taking this increase into consideration the inclusive branching ratio due to the  $c \rightarrow u\gamma$  short distance penguin reaches only the  $10^{-8}$  region, which is still much smaller than the effect of long distance contributions. Thus, in order to estimate these decays, one must concentrate on the treatment of the long distance dynamics involved in the  $D \rightarrow V\gamma$  transitions.

During the last few years several papers have appeared in which the  $D \rightarrow V\gamma$  transitions were considered. In ref. [3] the first comprehensive phenomenological study of the various  $D \rightarrow V\gamma$  has been presented, using mainly the techniques of pole diagrams and vector meson dominance. Other approaches include the use of the quark model picture and of effective Lagrangian [5, 6], the use of QCD sum rules [7] and the hybrid model approach, which combines heavy quark effective theory and chiral Lagrangian [8, 9, 10].

As it will be emphasized in the last section, the existing predictions of the various theoretical attempts are quite divergent for some of the  $D \rightarrow V\gamma$  modes which underlines the urgent need for experimental data as well as for the development of a reliable model.

It should also be mentioned that these decays offer certain opportunities to search for signals of physics beyond the standard model [9, 8, 11], although some of the proposed tests could be affected by the long distance contributions embodied in the  $c \rightarrow u\gamma$  transition [10].

In the present paper we aim for a more systematic and comprehensive treatment of these decays than previously undertaken, employing the formalism of the hybrid model [12, 13] for treating the  $D \rightarrow V\gamma$  transition [9, 10]. In Section 2, we present the details of our approach and we define the approximation used, in Section 3 we give the explicit form of the amplitudes and we conclude in Section 4 with a discussion and a comparative presentation of our numerical predictions.

## 2 Model description

We treat the radiative decays  $D \rightarrow V\gamma$  as originating from the non-leptonic transition  $D \rightarrow VV_0$ , followed by the conversion  $V_0 \rightarrow \gamma$  via the vector meson dominance mechanism. Although a similar scheme has been considered also in previous papers [3, 8, 10] there is no systematic treatment which includes all possible diagrams within the chosen approximation. In the present paper we adopt the factorization approach for the  $D \rightarrow VV_0$  amplitude, following the formalism advanced in [14] for the nonleptonic decays of  $D$ ,  $D_s$  mesons (BSW scheme). We shall not repeat here the arguments for using the factorization approximation, as these have been amply discussed in the literature (see, e.g. [14, 15]). We are aware that the nonfactorizable contributions could also play a role as it may be the case for certain D [16] and B [17] nonleptonic decays. However, at the present time, before any actual measurements of  $D \rightarrow V\gamma$  exist, we prefer to limit ourselves to a simple scheme, and to keep our approach as transparent as possible, awaiting the confrontation with experiment. The factorization amplitude for  $D \rightarrow VV_0$  in

BSW scheme is calculated using the effective nonleptonic weak Lagrangian

$$\mathcal{L}_w = -\frac{G_F}{\sqrt{2}}V_{uq_i}V_{cq_j}^* [a_1(\bar{u}q_i)^\mu(\bar{q}_j c)_\mu + a_2(\bar{u}c)_\mu(\bar{q}_j q_i)^\mu], \quad (1)$$

where  $(\bar{\psi}_1\psi_2)^\mu \equiv \bar{\psi}_1\gamma^\mu(1-\gamma^5)\psi_2$ ,  $q_{i,j}$  represent the fields of  $d$  or  $s$  quarks,  $V_{ij}$  are the CKM matrix elements and  $G_F$  is the Fermi constant. In our calculation we use  $a_1 = 1.26$  and  $a_2 = -0.55$  as found in [14].

In Eq. (1) the quark bilinears are treated as interpolating fields for the appropriate mesons. In order to calculate the matrix elements we use as before [8, 10] the hybrid model which combines the heavy quark effective and chiral perturbation theory [12, 13]. The relevant hadronic degrees of freedom within this framework are the charm pseudoscalar ( $D$ ) and vector ( $D^*$ ) mesons and the light pseudoscalar ( $P$ ) and vector ( $V$ ) mesons. In the factorization scheme ("vacuum insertion") which we use, the  $D \rightarrow VV_0$  amplitude is schematically approximated as follows

$$\begin{aligned} \langle VV_0|(\bar{q}_i q_j)^\mu(\bar{q}_k c)_\mu|D\rangle &= \langle V|(\bar{q}_i q_j)^\mu|0\rangle\langle V_0|(\bar{q}_k c)_\mu|D\rangle \\ &+ \langle V_0|(\bar{q}_i q_j)^\mu|0\rangle\langle V|(\bar{q}_k c)_\mu|D\rangle \\ &+ \langle VV_0|(\bar{q}_i q_j)^\mu|0\rangle\langle 0|(\bar{q}_k c)_\mu|D\rangle, \end{aligned} \quad (2)$$

where the first two terms are the spectator contributions, in the following denoted by  $A_{Spec,\gamma}$  and  $A_{Spec,V}$ , respectively, and the third term is the weak annihilation contribution, denoted by  $A_{Annih}$ .

In the three terms of Eq. (2), the  $V_0$  meson ( $\rho^0$ ,  $\omega$  and  $\Phi$ ) produced in the transition is allowed to convert into a photon through the vector meson dominance (VDM). The diagrams thus contributing to the amplitudes  $A_{Spec,\gamma}$ ,  $A_{Spec,V}$  and  $A_{Annih}$  are shown in the Figs. 1a, 1b and 1c, respectively. However, as a result of the specific form of the strong Lagrangian of the heavy particles (see Eqs. (11), (19) of [10]), there is also direct emission of the photon from the initial  $D$  meson, as exhibited in diagrams (C) and (D) of Fig. 1a.

The square in each diagram of Fig. 1 denotes the weak transition due to the effective Lagrangian  $\mathcal{L}_w$  (1). This Lagrangian contains a product of

two left handed quark currents  $(\bar{\psi}_1\psi_2)^\mu$ , each denoted by a dot on Fig. 1. In our model, the left handed currents will be expressed in terms of the relevant hadronic degrees of freedom:  $D$ ,  $D^*$ ,  $P$  and  $V$ . In our notation in the diagram (B), for example, the hadronic current  $J_2$  creates  $V$  meson, while the hadronic current  $J_1$  annihilates  $D$  and creates  $V_0$  at the same time.

In ref. [10] (FS) which also uses the hybrid model for these decays, most diagrams exhibited in Fig. 1 have already been calculated. We shall not repeat this calculation here and shall combine the results of FS with those of our systematic approach, to obtain the full  $D \rightarrow V\gamma$  amplitude in the factorization approximation. We rely on FS as a complementary source for various basic expressions giving here only those formulae which are directly necessary for the calculations of the present paper.

The principal contribution missing in FS is due to diagram (B) of Fig. 1a. As it turns out, the inclusion of this parity - violating (PV) contribution, alters considerably the numerical values of the FS amplitudes in the PV sector and leads to the set of predictions for these decays exhibited in Table 2, which will be discussed in the last Section. The relevant expressions needed for diagram (B) are given below.

The weak current  $J_1$  of diagram (B) (see Fig. 1) annihilates quark  $c$  and creates one of the light quarks  $q$  ( $u$ ,  $d$  or  $s$ ):  $J_1^\mu = \bar{q}\gamma^\mu(1 - \gamma^5)c$ . Under chiral  $SU(3)_L \times SU(3)_R$  this quark current transform as  $(\bar{3}_L, 1_R)$ . At the hadronic level we impose the same chiral transformation and we require the current to be linear in the heavy meson fields  $D^a$  and  $D_\mu^{*a}$  [18, 12, 13]

$$\begin{aligned}
J_{1a}^\mu = & \frac{1}{2} i\alpha Tr[\gamma^\mu(1 - \gamma_5)H_b u_{ba}^\dagger] \\
& + \alpha_1 Tr[\gamma_5 H_b(\hat{\rho}^\mu - \mathcal{V}^\mu)_{bc} u_{ca}^\dagger] \\
& + \alpha_2 Tr[\gamma^\mu \gamma_5 H_b v_\alpha(\hat{\rho}^\alpha - \mathcal{V}^\alpha)_{bc} u_{ca}^\dagger] + \dots, \quad (3)
\end{aligned}$$

where  $\alpha = f_H\sqrt{m_H}$  and  $\alpha_1$  and  $\alpha_2$  are free parameters, which have to be determined from the experiment. The current (3) is the most general one in the leading  $1/m_c$  order of HQET and next to leading order of chiral perturbation theory [18, 12, 13]. Here both the heavy pseudoscalar and the heavy

vector mesons were incorporated in a  $4 \times 4$  matrix  $H_a$

$$H_a = \frac{1}{2}(1+\not{v})(P_{a\mu}^*\gamma^\mu - P_a\gamma_5), \quad (4)$$

where  $a = 1, 2, 3$  is the  $SU(3)_V$  index of the light flavours, and  $P_{a\mu}^*$ ,  $P_a$ , annihilate a spin 1 and spin 0 heavy meson  $Q\bar{q}_a$  of velocity  $v$ , respectively. The fields  $\mathcal{V}$  and  $u$  incorporate the light pseudoscalars and are given in FS. The field  $\hat{\rho}$  incorporates the light vector mesons

$$\hat{\rho}_\mu = i\frac{\tilde{g}_V}{\sqrt{2}}\rho_\mu, \quad \rho_\mu = \begin{pmatrix} \frac{\rho_\mu^0 + \omega_\mu}{\sqrt{2}} & \rho_\mu^+ & K_\mu^{*+} \\ \rho_\mu^- & \frac{-\rho_\mu^0 + \omega_\mu}{\sqrt{2}} & K_\mu^{*0} \\ K_\mu^{*-} & \bar{K}_\mu^{*0} & \Phi_\mu \end{pmatrix}. \quad (5)$$

where  $\tilde{g}_V = 5.9$  was fixed in the case of exact flavour symmetry (see e.g. references in FS).

The weak current  $J_2$  of diagram (B) (see Fig. 1) creates the final  $V$  meson. Its matrix elements are given by [10]

$$\langle V(\epsilon_V, q) | J_{2\mu} | 0 \rangle = \epsilon_\mu^*(q) g_V(q^2), \quad (6)$$

where the couplings  $g_V(m_V^2)$  are measured in the leptonic decays of the mesons:  $g_\rho(m_\rho^2) \simeq g_\rho(0) = 0.17 \text{ GeV}^2$ ,  $g_\omega(m_\omega^2) \simeq g_\omega(0) = 0.15 \text{ GeV}^2$ ,  $g_\Phi(m_\Phi^2) \simeq g_\Phi(0) = 0.24 \text{ GeV}^2$  and  $g_{K^*} = (m_{K^*}/m_\rho)g_\rho$ .

For the calculation of the amplitude, we also need the  $\gamma - V_0$  interaction Lagrangian, given by the vector meson dominance like in [8, 10]

$$\mathcal{L}_{V\gamma} = -\frac{e}{\sqrt{2}}B_\mu(g_\rho\rho^{0\mu} + \frac{g_\omega}{3}\omega^\mu - \frac{\sqrt{2}g_\Phi}{3}\Phi^\mu), \quad (7)$$

where  $B_\mu$  is the photon field.

### 3 Decay amplitudes

In order to facilitate the incorporation of the results of FS we shall adopt here their notation of the amplitudes, namely  $A_{PC}^i$ ,  $A_{PV}^i$  for the parity - conserving and parity - violating parts, where  $i$  denotes classes of diagrams

identified below. The general gauge invariant amplitude  $D(p) \rightarrow V(p_V)\gamma(q)$  is

$$\begin{aligned}
A(D(p) \rightarrow V(\epsilon_{(V)}, p_{(V)})\gamma(\epsilon_{(\gamma)}, q)) &= e \frac{G_F}{\sqrt{2}} V_{uq_i} V_{cq_j}^* \{ \epsilon_{\mu\nu\alpha\beta} q^\mu \epsilon_{(\gamma)}^{*\nu} p^\alpha \epsilon_{(V)}^{*\beta} A_{PC} \\
&\quad + i[(\epsilon_{(V)}^* \cdot q)(\epsilon_{(\gamma)}^* \cdot p_{(V)}) - (p_{(V)} \cdot q)(\epsilon_{(V)}^* \cdot \epsilon_{(\gamma)}^*)] A_{PV} \}, \quad (8)
\end{aligned}$$

with  $A_{PC} = A_{PC}^I + A_{PC}^{II} + A_{PC}^{III}$  and  $A_{PV} = A_{PV}^I + A_{PV}^{II} + A_{PV}^{III}$ . Now, concerning the classification of diagrams,  $A_{PC}^I$  will denote the contribution from diagrams (A) and (C) (see Fig. 1) which encompass the  $D^* \rightarrow D\gamma$  transition, while  $A_{PC}^{II}$  will denote diagram (G) which contains the  $P \rightarrow V\gamma$  transition.  $A_{PC}^{III}$ ,  $A_{PV}^{III}$  denote the contribution of the long distance penguins described by Fig. 1 of FS. On the hadronic level they are represented by the diagrams (E) and (F), respectively, and they vanish in the exact SU(3) flavour limit as shown in FS. We also define two other classes of parity violating diagrams:  $A_{PV}^I$  will include the bremsstrahlung-like diagrams (D) and (H), whereby the photon emission is due to the direct coupling to charged initial D or final V mesons. Finally,  $A_{PV}^{II}$ , which has not been studied before, will denote the contribution represented by the diagram (B). As this contribution will be considered in detail below, we present its quark level picture in Fig. 2: Fig. 2a represents the diagram (B) for the decays proportional to  $a_1$ , for example  $D_s^+ \rightarrow \rho^+\gamma$ , while Fig. 2b represents the decays proportional to  $a_2$ , for example  $D_0 \rightarrow \bar{K}^{*0}\gamma$ .

Now we turn to the calculation of the amplitude for the diagram (B), while the remaining contributions have been studied in FS. First we parametrize the matrix element  $\langle V_0 | J_1^\mu | D \rangle$  in the usual way [19]

$$\begin{aligned}
&\langle V_0(q, \epsilon_{V_0}) | J_1^\mu | D(p) \rangle = \quad (9) \\
&= \frac{2V(Q^2)}{m_D + m_{V_0}} \epsilon^{\mu\nu\alpha\beta} \epsilon_{V_0\nu}^* p_\alpha q_\beta + i2 \frac{\epsilon_{V_0}^* \cdot Q}{Q^2} m_{V_0} Q^\mu (A_3(Q^2) - A_0(Q^2)) \\
&\quad + i(m_D + m_{V_0}) \left[ \epsilon_{V_0}^{\mu*} A_1(Q^2) - \frac{\epsilon_{V_0}^* \cdot Q}{(m_D + m_{V_0})^2} (p + q)^\mu A_2(Q^2) \right],
\end{aligned}$$

where  $Q = p - q$ . In fact the diagram (B) contributes only to form factors  $A_0$ ,  $A_1$ ,  $A_2$  and  $A_3$ , which will be determined using the model described above. The form factor  $V(Q^2)$  gets contribution from the diagrams (A) and (C) of

Fig.1, its results are explained in FS, therefore we will leave this contribution aside here. In order that these matrix elements be finite at  $Q^2 = 0$ , the form factors satisfy the relation [19]

$$A_3(Q^2) - \frac{m_D + m_{V0}}{2m_{V0}}A_1(Q^2) + \frac{m_D - m_{V0}}{2m_{V0}}A_2(Q^2) = 0, \quad (10)$$

and  $A_3(0) = A_0(0)$ .

Using the currents (6) and (9) and the relation (10) we determine the amplitude of the diagram (B) for  $D_s^+ \rightarrow \rho^+ \Phi$  as an example:

$$\begin{aligned} \mathcal{A}_{PV}(D_s^+(p) \rightarrow \rho^+(p_{(V)}, \epsilon_{(V)})\Phi(q, \epsilon_{(\Phi)})) &= \frac{G_F}{\sqrt{2}}a_1V_{cs}^*V_{ud}(m_D + m_\Phi) \\ &\times \left( \epsilon_{(\Phi)}^{*\mu} A_1(m_V^2) - \frac{(\epsilon_{(\Phi)}^* \cdot p_{(V)})}{(m_D + m_\Phi)^2}(p + q)^\mu A_2(m_V^2) \right) g_V \epsilon_{(V)\mu}^*. \end{aligned} \quad (11)$$

According to the vector meson dominance (7), the amplitude for  $D_s^+ \rightarrow \rho^+ \gamma$  is obtained, if the polarization  $\epsilon_{(\Phi)}^{*\mu}$  is replaced by  $\epsilon_{(\gamma)}^{*\mu} e g_\Phi / (3m_\Phi^2)$ . However, the amplitude for  $D_s^+ \rightarrow \rho^+ \gamma$  decay should satisfy the gauge invariance condition. It was found [20, 21] for the case of  $B \rightarrow K^* \gamma$  decay, that it is useful to analyze the heavy meson decays into  $VV_0$  in terms of helicity amplitudes of the two final vector meson:  $\mathcal{A}_{++}$ ,  $\mathcal{A}_{--}$  and  $\mathcal{A}_{00}$ . Thus, the application of gauge invariance condition to  $D \rightarrow VV_0$  decay, with  $V_0 \rightarrow \gamma$  conversion, means that the  $\mathcal{A}_{00}(D \rightarrow VV_0)$  helicity amplitude must be discarded. Under a gauge transformation as implemented by  $\epsilon_{(\gamma)}^\mu \rightarrow q^\mu$ , we derive the following general condition for the  $D \rightarrow VV_0 \rightarrow V\gamma$  decays

$$\sum_{V^0} (m_D + m_{V^0}) \left[ A_1(m_V^2) - \frac{m_D^2 - m_V^2}{(m_D + m_{V^0})^2} A_2(m_V^2) \right] = 0 \quad (12)$$

imposed for the decays of type (B) graphs, presented on Fig. 1a. Consequently, the  $A_{PV}^I$  amplitude can be expressed in terms of the form factor  $A_1(m_V^2)$  only.

Now we determine the form factors  $A_1(m_V^2)$  for the diagram (B) using the current (3) and parametrizing it in the form of (9). The weak current (3) determines the form factor in the heavy quark limit, i.e. at the maximum



momentum transfer  $Q_{max}^2 = (m_D - m_{V0})^2$

$$A_1^{DV_0}(Q_{max}^2) = -\frac{\tilde{g}_V}{\sqrt{2}} 2\alpha_1 \frac{\sqrt{m_D}}{m_D + m_{V0}}. \quad (13)$$

We assume the pole dominance behaviour of the form factors [12, 13] and at  $Q^2 = m_V^2$  we determine

$$A_1^{DV_0}(m_V^2) = -\tilde{g}_V \sqrt{2} \alpha_1 \frac{\sqrt{m_D}}{m_D + m_{V0}} \frac{1 - \frac{(m_D - m_{V0})^2}{m_{D_1^+}^2}}{1 - \frac{(m_V)^2}{m_{D_1^+}^2}}, \quad (14)$$

where  $D_{1^+}$  is the mass of the  $\bar{q}c$   $J^P = 1^+$  bound state. We use the masses of  $\bar{s}c$  and  $\bar{d}c$  bound states to be  $2.53 \text{ GeV}$  and  $2.42 \text{ GeV}$  as in [13]. The free parameter  $\alpha_1$  is determined by using the average of experimental  $A_1(0)$  values for  $D_s^+ \rightarrow \Phi l \nu_l$  and  $D^+ \rightarrow \bar{K}^{*0} l \nu_l$ . We obtain  $|\alpha_1| = 0.171 \text{ GeV}^{1/2}$  and use this value for the prediction of all  $D \rightarrow V \gamma$  decay rates.

Using the formalism described above, with Eqs.(11), (12), (14), we obtain  $A_{PV}^{II}$  for the various decay channels.

The Cabibbo allowed decay amplitudes, which are proportional to the product  $|V_{ud}V_{cs}^*|$ , are:

$$\begin{aligned} A_{PV}^{II}(D^0 \rightarrow \bar{K}^{*0} \gamma) &= -a_2 \left[ \frac{g_\rho g_{K^*}}{m_\rho^2} (m_D + m_\rho) |A_1^{D\rho}(m_{K^*}^2)| \right. \\ &\quad \left. + \frac{g_\omega g_{K^*}}{3m_\omega^2} (m_D + m_\omega) |A_1^{D\omega}(m_{K^*}^2)| \right] \frac{1}{m_D^2 - m_{K^*}^2} \quad (15) \end{aligned}$$

$$A_{PV}^{II}(D_s^+ \rightarrow \rho^+ \gamma) = a_1 \frac{2g_\Phi g_\rho}{3m_\Phi} (m_D + m_\Phi) |A_1^{D_s \Phi}(m_\rho^2)| \frac{1}{m_{D_s}^2 - m_\rho^2}. \quad (16)$$

The Cabibbo suppressed amplitudes  $A_{PV}^{II}$  proportional to the Cabibbo factor  $|V_{su}V_{cs}^*|$  are

$$\begin{aligned} A_{PV}^{II}(D^+ \rightarrow \rho^+ \gamma) &= -a_1 \left[ \frac{g_\rho^2}{m_\rho^2} (m_D + m_\rho) |A_1^{D\rho}(m_\rho^2)| \right. \\ &\quad \left. - \frac{g_\omega g_\rho}{3m_\omega^2} (m_D + m_\omega) |A_1^{D\omega}(m_\rho^2)| \right] \frac{1}{m_D^2 - m_\rho^2} \quad (17) \end{aligned}$$

$$A_{PV}^{II}(D_s^+ \rightarrow K^{*+}\gamma) = a_1 \frac{2g_\Phi g_{K^*}}{3m_\Phi} (m_{D_s} + m_\Phi) |A_1^{D_s\Phi}(m_{K^*}^2)| \frac{1}{m_{D_s}^2 - m_{K^*}^2} \quad (18)$$

$$\begin{aligned} A_{PV}^{II}(D^0 \rightarrow \rho^0\gamma) &= -\frac{a_2}{\sqrt{2}} \left[ \frac{g_\rho^2}{m_\rho^2} (m_D + m_\rho) |A_1^{D\rho}(m_\rho^2)| \right. \\ &\quad \left. + \frac{g_\omega g_\rho}{3m_\omega^2} (m_D + m_\omega) |A_1^{D\omega}(m_\rho^2)| \right] \frac{1}{m_D^2 - m_\rho^2}. \quad (19) \end{aligned}$$

$$\begin{aligned} A_{PV}^{II}(D^0 \rightarrow \omega\gamma) &= \frac{a_2}{\sqrt{2}} \left[ \frac{g_\rho^2}{m_\rho^2} (m_D + m_\rho) |A_1^{D\rho}(m_\omega^2)| \right. \\ &\quad \left. + \frac{g_\rho g_\omega}{3m_\omega^2} (m_D + m_\omega) |A_1^{D\omega}(m_\omega^2)| \right] \frac{1}{m_D^2 - m_\omega^2}. \quad (20) \end{aligned}$$

$$\begin{aligned} A_{PV}^{II}(D^0 \rightarrow \Phi\gamma) &= -a_2 \left[ \frac{g_\rho g_\Phi}{m_\rho^2} (m_D + m_\rho) |A_1^{D\rho}(m_\Phi^2)| \right. \\ &\quad \left. + \frac{g_\omega g_\Phi}{3m_\omega^2} (m_D + m_\omega) |A_1^{D\omega}(m_\Phi^2)| \right] \frac{1}{m_D^2 - m_\Phi^2}. \quad (21) \end{aligned}$$

For completeness, we give also the parity violating parts of the amplitudes for doubly suppressed decays proportional to  $|V_{us}V_{cd}^*|$ :

$$\begin{aligned} A_{PV}^{II}(D^+ \rightarrow K^{*+}\gamma) &= -a_1 \left[ \frac{g_\rho g_{K^*}}{m_\rho^2} (m_D + m_\rho) |A_1^{D\rho}(m_{K^*}^2)| \right. \\ &\quad \left. - \frac{g_\omega g_{K^*}}{3m_\omega^2} (m_D + m_\omega) |A_1^{DK^*}(m_{K^*}^2)| \right] \frac{1}{m_D^2 - m_{K^*}^2}, \quad (22) \end{aligned}$$

$$\begin{aligned} A_{PV}^{II}(D^0 \rightarrow K^{*0}\gamma) &= a_2 \left[ \frac{g_\rho g_{K^*}}{m_\rho^2} (m_D + m_\rho) |A_1^{D\rho}(m_{K^*}^2)| \right. \\ &\quad \left. + \frac{g_\omega g_{K^*}}{3m_\omega^2} (m_D + m_\omega) |A_1^{D\omega}(m_{K^*}^2)| \right] \frac{1}{m_D^2 - m_{K^*}^2}. \quad (23) \end{aligned}$$

## 4 Discussion

We present numerical results for the amplitudes  $\mathcal{A}_{PC}^I$ ,  $\mathcal{A}_{PC}^{II}$ ,  $\mathcal{A}_{PC}^{III}$ ,  $\mathcal{A}_{PV}^I$ ,  $\mathcal{A}_{PV}^{II}$  and  $\mathcal{A}_{PV}^{III}$  in Table 1, where  $\mathcal{A}^i$  denotes

$$\mathcal{A}_{PC(V)}^i = e \frac{G_F}{\sqrt{2}} V_{uq_j} V_{cq_k}^* \mathcal{A}_{PC(V)}^i. \quad (24)$$

and  $i$  runs over the nine decays studied. The amplitudes  $\mathcal{A}_{PC}^{II}$  are calculated from Eqs. (15) - (23), while for the rest of the amplitudes we use the values obtained in FS. Although we have the values of Table 1, which encompass all the amplitudes arising from our factorization scheme and hybrid model, we cannot predict at this stage definite values for the decay rates. This is due to the fact that the signs of several constants entering the expressions of  $\mathcal{A}_{PC}^i$ ,  $\mathcal{A}_{PV}^i$  (like  $\lambda'$ ,  $\lambda$ ,  $C_{VV\Pi}$ ,  $g_V$ ,  $\alpha_1$ , defined in FS and here) are not determined yet from the experimental data. Thus, we must contain ourselves in the present only to the range of values, which are obtained by assuming all possible relative signs for the various constants. We also remark that  $\mathcal{A}_{PC}^{III}$ ,  $\mathcal{A}_{PV}^{III}$  are usually one to two orders of magnitude smaller than the other amplitudes and will affect the rates only in the case of cancellations occurring among the rest of amplitudes.

We calculate the branching ratios of the  $D \rightarrow V\gamma$  decays with the help of

$$\Gamma(D \rightarrow V\gamma) = \frac{1}{4\pi} \left[ \frac{m_D^2 - m_V^2}{2m_D} \right]^3 (|\mathcal{A}_{PC}|^2 + |\mathcal{A}_{PV}|^2), \quad (25)$$

and we present the possible range of values for the branching ratios in Table 2. We compare the present results, denoted by (a), with the results obtained in previous approaches. The results of the approach [10] are denoted by (b), the results of [3] by (c), and the results of [7] by (d) (we specify  $a_1 = 1.26$  and  $a_2 = -0.55$  in their formulas). The quark model calculation of [5] predicts the branching ratio for the Cabibbo allowed decays  $BR(D^0 \rightarrow \bar{K}^{*0}\gamma) = 8.6 \cdot 10^{-6}$  and  $BR(D_s^+ \rightarrow \rho^+\gamma) = 2.1 \cdot 10^{-5}$ , which are smaller in comparison with the results we obtain here, as well as compared with the predictions of [3] and

[10]. On the other hand, the calculation of [6], which also uses a quark model, leads to a larger branching ratio  $BR(D^0 \rightarrow \bar{K}^{*0}\gamma) = 1.1 \cdot 10^{-4}$ , which is an order of magnitude larger than obtained in [5] and closer to our estimate. We notice that the parity violating amplitudes calculated within the present approach have changed significantly in comparison with the results of FS. Overall, inspection of Table 2, indicates that our predictions in the present paper are closest to those of [3]. When measurements of a few channels will be available it will be possible to adjust the range of the various branching ratios and to make firmer predictions, hopefully allowing to select the best suited model.

The measurable ratio  $\mathcal{A}_{PC}/\mathcal{A}_{PV}$  can also be used to distinguish between the various models. However, since at the present stage we cannot specify the relative signs of the various components of each of these amplitudes, we are unable to make any sensible statement about these ratios.

We summarize our results as follows: we have presented a calculation of the radiative  $D \rightarrow V\gamma$  decays using a model which contains all classes of diagrams arising from the factorization approach for the  $D \rightarrow VV^0$  amplitude, from which the radiative decays are obtained by use of vector meson dominance. In the calculations of the various matrix elements, we use a hybrid model [12, 13] which combines heavy quark techniques with the chiral Lagrangian. In view of uncertainties related to the coupling constants involved, we can predict at this stage only ranges for the branching ratios of the various decay channels, which are given in Table 2. We emphasize that the Cabibbo allowed decays  $D^0 \rightarrow \bar{K}^{*0}\gamma$  and  $D_s^+ \rightarrow \rho^+\gamma$  are calculated to be fairly frequent, with branching ratios of a few times  $10^{-4}$  and we expect their detection soon. Some of the Cabibbo suppressed modes, like  $D^{+,0} \rightarrow \rho^{+,0}\gamma$  may also occur with branching ratios close to  $10^{-4}$ . Experimental results on these modes are eagerly awaited and will certainly contribute to clarify the long distance dynamics leading to these radiative decays.

*Acknowledgements:* The research of S.F. and S.P. was supported in part by the Ministry of Science of the Republic of Slovenia. The research of P.S. was supported in part by Fund for Promotion of Research at the Technion.

## References

- [1] M. Selen: Bull. Am. Phys. Soc. 39 (1994) 1147
- [2] S. Ratti: private communication on experiment E831 - FOCUS
- [3] G. Burdman, E. Golowich, J. L. Hewett and S. Pakvasa: Phys. Rev. D 52 (1995) 6383
- [4] G. Greub, T. Hurth, M. Misiak and D. Wyler: Phys. Lett. B 382 (1996)415
- [5] P. Asthana and A. N. Kamal: Phys. Rev. D 43 (1991) 278
- [6] H.-Y. Cheng et al.: Phys. Rev. D 51 (1995) 1199
- [7] A. Khodjamirian, G. Stoll, D. Wyler: Phys. Lett. B 358 (1995) 129
- [8] B. Bajc, S. Fajfer and R.J. Oakes: Phys. Rev. D 51 (1995) 2230
- [9] B. Bajc, S. Fajfer and R. J. Oakes: Phys. Rev. D 54 (1996) 5883
- [10] S. Fajfer and P. Singer: Phys. Rev. D 56 (1997) 4302
- [11] I. I. Bigi, F. Gabbiani and A. Masiero: Z. Phys. C 48 (1990) 633; I. I. Bigi: CERN-TH. 7370/94 (unpublished) and UND-HEP-95B1608, hep-ph/9508294
- [12] R. Casalbuoni et al.: Phys. Lett. B 292 (1992) 371
- [13] R. Casalbuoni et al.: Phys. Lett. B 299 (1993) 139
- [14] M. Bauer, B. Stech and M. Wirbel: Z. Phys. C 34 (1987) 103
- [15] A. J. Buras: Nucl. Phys. B 434 (1995) 606
- [16] A. N. Kamal et al.: Phys. Rev. D 53 (1996) 2506
- [17] J. M. Soares: Phys. Rev. D 51 (1995) 3518; K. Terasaki: Phys. Rev. D 54 (1996) 3649; Kyoto University Report YITP-97-52 (unpublished)

- [18] B. Bajc, S. Fajfer and R. J. Oakes: Phys. Rev. D 53 (1996) 4957
- [19] M. Bauer, B. Stech and M. Wirbel: Z. Phys. C 29 (1985) 637
- [20] E. Golowich and S. Pakvasa: Phys. Rev. D 51 (1995) 1215
- [21] J. M. Soares: Phys. Rev. D 53 (1996) 241

### Figure Captions

**Fig. 1.** Skeleton diagrams of various contributions to the long distance decay  $D \rightarrow V\gamma$ . The spectator diagrams of type  $A_{Spec,\gamma}$  (see Eq. (2) in the text) are shown in Fig. 1a, the spectator diagrams of type  $A_{Spec,V}$  are shown in Fig. 1b and the weak annihilation diagrams  $A_{Annih}$  are shown in Fig. 1c. The square in each diagram denotes the weak transition due to the effective Lagrangian  $\mathcal{L}_w$  (1). This Lagrangian contains a product of two left handed quark currents  $(\bar{\psi}_1\psi_2)^\mu$ , each denoted by a dot. Different diagrams are denoted by (A) - (H). Their contributions to the amplitudes  $\mathcal{A}_{PC}^i$  and  $\mathcal{A}_{PV}^i$  are specified in the text.

**Fig. 2.** The quark level picture of the diagram (B) of Fig. 1 (amplitude  $A_{PV}^H$ ): Fig. 2a represents the decays proportional to  $a_1$ , for example  $D_s^+ \rightarrow \rho^+\gamma$ , while Fig. 2b represents the decays proportional to  $a_2$ , for example  $D_0 \rightarrow \bar{K}^{*0}\gamma$ .

$D \rightarrow V\gamma$	$ \mathcal{A}_{PC}^I $	$ \mathcal{A}_{PC}^{II} $	$ \mathcal{A}_{PC}^{III} $	$ \mathcal{A}_{PV}^I $	$ \mathcal{A}_{PV}^{II} $	$ \mathcal{A}_{PV}^{III} $
$D^0 \rightarrow K^{*0}\gamma$	6.4	6.2	0	0	5.5	0
$D_s^+ \rightarrow \rho^+\gamma$	1.4	7.3	0	7.4	4.3	0
$D^0 \rightarrow \rho^0\gamma$	0.82	1.0	0.02	0	0.71	0.03
$D^0 \rightarrow \omega\gamma$	0.73	1.07	0.02	0	0.63	0.03
$D^0 \rightarrow \Phi\gamma$	1.8	1.34	0	0	1.8	0
$D^+ \rightarrow \rho^+\gamma$	0.59	1.3	0.02	1.6	1.3	0.03
$D_s^+ \rightarrow K^{*+}\gamma$	0.41	2.3	0.02	2.1	1.2	0.04
$D^+ \rightarrow K^{*+}\gamma$	0.16	0.42	0	0.43	0.37	0
$D^0 \rightarrow K^{*0}\gamma$	0.33	0.32	0	0	0.28	0

Table 1: The parity conserving and parity violating amplitudes for charm meson decays in units  $10^{-8} GeV^{-1}$ . The amplitudes  $\mathcal{A}_{PC,PV}^i$  get contributions from different diagrams in Fig. 1: (A) and (C) contribute to  $\mathcal{A}_{PC}^I$ , (D) and (H) contribute to  $\mathcal{A}_{PV}^I$ , (G), (B), (E) and (F) contribute to  $\mathcal{A}_{PC}^{II}$ ,  $\mathcal{A}_{PV}^{II}$ ,  $\mathcal{A}_{PC}^{III}$  and  $\mathcal{A}_{PV}^{III}$ , respectively. The amplitudes  $\mathcal{A}_{PC}^I$ ,  $\mathcal{A}_{PC}^{II}$ ,  $\mathcal{A}_{PC}^{III}$ ,  $\mathcal{A}_{PV}^I$  and  $\mathcal{A}_{PV}^{III}$  were calculated in [10], while the amplitude  $\mathcal{A}_{PV}^{II}$  represents the additional contribution calculated here. The first two decays are Cabibbo allowed, while the last two are doubly Cabibbo suppressed.

$D \rightarrow V\gamma$	$BR(a) \times 10^5$	$BR(b) \times 10^5$	$BR(c) \times 10^5$	$BR(d) \times 10^5$
$D^0 \rightarrow K^{*0}\gamma$	(6 – 36)	( $10^{-2}$ – 30)	(7 – 12)	0.18
$D_s^+ \rightarrow \rho^+\gamma$	(20 – 80)	(34 – 50)	(6 – 38)	4.4
$D^0 \rightarrow \rho^0\gamma$	(0.1 – 1)	(0.02 – 1)	(0.1 – 0.5)	0.38
$D^0 \rightarrow \omega\gamma$	(0.1 – 0.9)	(0.02 – 0.8)	$\simeq 0.2$	–
$D^0 \rightarrow \Phi\gamma$	(0.4 – 1.9)	(0.04 – 1.6)	(0.1 – 3.4)	–
$D^+ \rightarrow \rho^+\gamma$	(0.4 – 6.3)	(1.8 – 4.1)	(2 – 6)	0.43
$D_s^+ \rightarrow K^{*+}\gamma$	(1.2 – 5.1)	(2.1 – 3.2)	(0.8 – 3)	–
$D^+ \rightarrow K^{*+}\gamma$	(0.03 – 0.44)	(0.12 – 0.25)	0.1 – 0.3	–
$D^0 \rightarrow K^{*0}\gamma$	(0.03 – 0.2)	( $10^{-5}$ – 0.08)	$\simeq 0.01$	–

Table 2: The branching ratios for  $D \rightarrow V\gamma$  decays. The first column (a) contains the results of the present approach. The next three columns present the results of Ref. [10] (b), Ref. [3] (c), and Ref. [7] (d). The first two decays are Cabibbo allowed, while the last two are doubly Cabibbo suppressed.



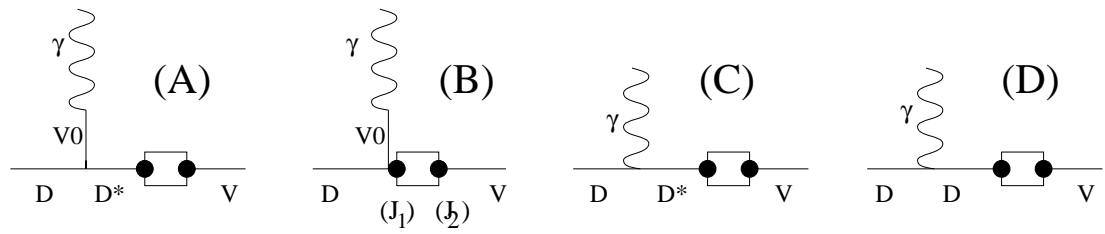


Fig. 1a

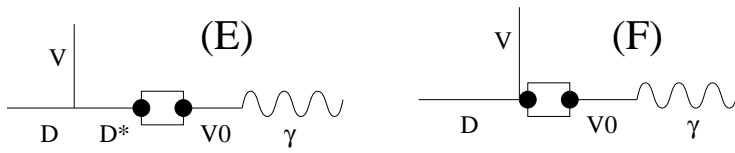


Fig. 1b

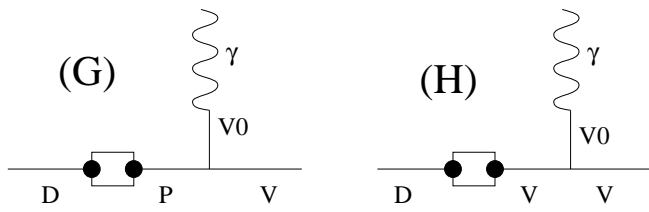


Fig. 1c

Fig. 1

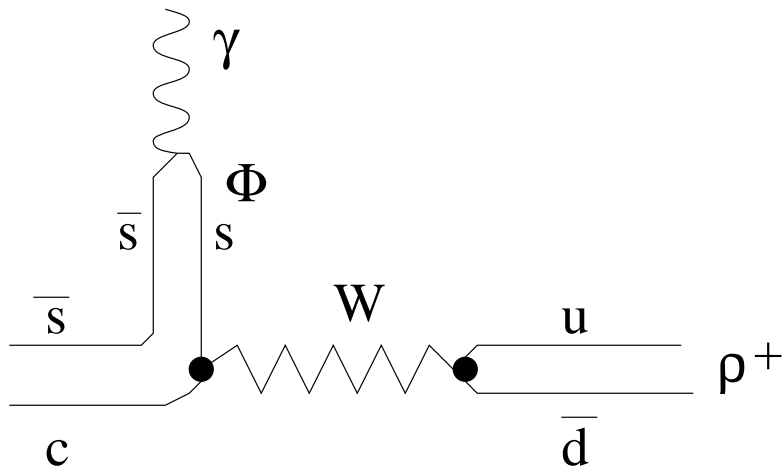


Fig. 2a:  $D_s^+ \rightarrow \rho^+ \gamma$

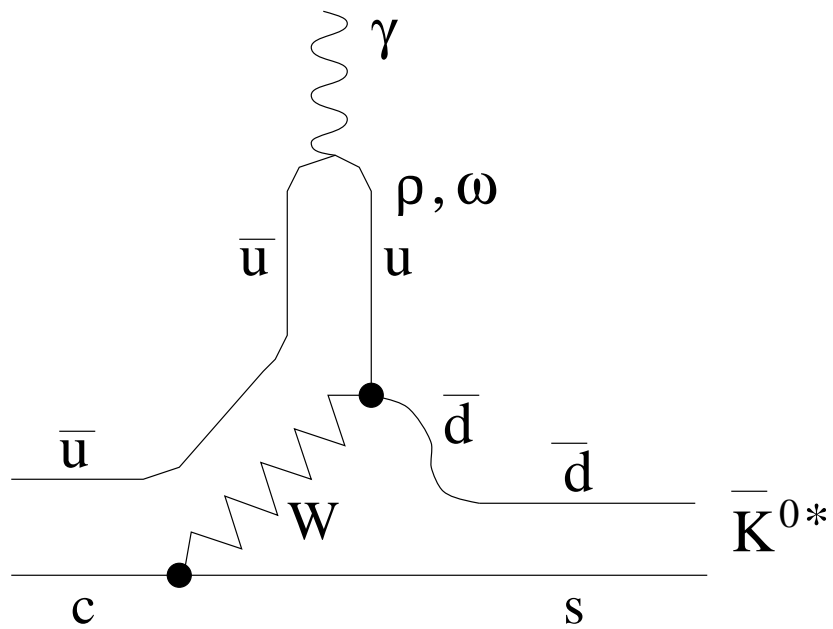


Fig. 2b:  $D^0 \rightarrow \bar{K}^{0*} \gamma$

Fig. 2